Vehicle-based Sensing for Energy and Emission Reduction

Center for Transportation, Environment, and Community Health

Final Report

by

Xiaopeng Li, Zhaohui Liang, Xiaowei Shi, Handong Yao

December 14, 2021

DISCLAIMER

TECHNICAL REPORT STANDARD TITLE PAGE

1. Report No.	2.Government Accession No.	3. Recipient's Catalog No.
4. Title and Subtitle Vehicle-based Sensing for Energy and Emission Reduction		5. Report Date December 14, 2021 6. Performing Organization Code
7. Author(s) Xiaopeng Li, Zhaohui Liang, Xiaowei Shi, Handong Yao		8. Performing Organization Report No.
9. Performing Organization Name and Address Department of Civil and Environmental Engineering University of South Florida Tampa, FL, 33620		10. Work Unit No. 11. Contract or Grant No. 69A3551747119
12. Sponsoring Agency Name and Address U.S. Department of Transportation 1200 New Jersey Avenue, SE Washington, DC 20590		13. Type of Report and Period Covered Final Report 07/01/2020-09/30/2021 14. Sponsoring Agency Code US-DOT
15. Supplementary Notes		

16. Abstract

Emerging automated vehicles (AV) may be able to provide advanced information about the surrounding information with video cameras, radar sensors, lidar sensors, etc. Such information will enable estimating and predicting transportation system states on mobility, energy, and emissions. In this study, a physical informed neural network is developed to perform an accurate tire-road friction estimation by utilizing those advanced vehicle sensors. A runway friction tester is employed as the ground truth. More than 15,000 GPS date points and other vehicle dynamic data points are collected during the field experiment, as a result, short convergence time and desired prediction accuracy are achieved by introducing the magic tire model and the slip-slop factor into the loss function.

17. Key Words	18. Distribution Statement
Autonomous Vehicle, Vehicle-based sensing, Pavement sensing	

19. Security Classif (of this report)	20. Security Classif. (of this page)	21. No of Pages	22. Price
Unclassified	Unclassified		

Form DOT F 1700.7 (8-69)

Abstract

Emerging automated vehicles (AV) may be able to provide advanced information about the surrounding information with video cameras, radar sensors, lidar sensors, etc. Such information will enable estimating and predicting transportation system states on mobility, energy, and emissions. In this study, a physical informed neural network is developed to perform an accurate tire-road friction estimation by utilizing those advanced vehicle sensors. A runway friction tester is employed as the ground truth. More than 15,000 GPS date points and other vehicle dynamic data points are collected during the field experiment, As a result, short convergence time and desired prediction accuracy are achieved by introducing the magic tire model and the slip-slop factor into the loss function.

Introduction

Vehicle technologies have undergone drastic improvements in recent years, in particular on sensing technologies that report a variety of vehicle and environment conditions and control technologies that automate vehicle driving. For example, many existing production vehicles are furnished with sensors that can record vehicles' operational states, including speed, fuel consumption, steering angle, and each individual tire speed. Further, recently emerging automated vehicles (AV) may be able to provide advanced information about the surrounding information with video cameras, radar sensors, lidar sensors, etc. On the other hand, connected vehicle (CV) technology that enables communications between vehicles and roadside infrastructure provides the communication platform to integrate sensor information from multiple vehicles or even a traffic stream. Such information will enable estimating and predicting transportation system states on mobility, energy, and emissions. Further, it will help better control AVs to smooth traffic and reduce system energy consumption and emissions, thereby improving the environment and community health.

To date, a series of studies have investigated this possibility [1], [2]. Qu et al. [3] developed a car-following model for electric and connected AVs based on reinforcement learning to dampen traffic oscillations and reduce fuel consumption. Yao et al. [4] proposed a trajectory smoothing method for connected AVs. In their study, with real-time traffic demand and signal timing information, connected AVs are optimized to run smoothly without any full stop and thus reduce fuel consumption. Li et al. [5] studied a periodic switching control method for an AV platoon to minimize the overall fuel consumption. Wadud et al. [6] explored the net effects of AVs on fuel consumption and greenhouse emissions. They found that AVs might plausibly reduce road transport greenhouse gas emissions and energy use by nearly half in some scenarios. This project will set up a framework for utilizing vehicle-based sensing information to assist AV driving and traffic control, aiming to bring in mobility and environmental benefits.

For the safe operation of the vehicle on the road, active and passive vehicle stability control system, such as Traction Control System (TCS) and Anti-lock Braking System (ABS) has been widely employed by various manufacturers. Those systems rely greatly on the accurate estimation of the tire-road friction factor. However, considering the cost and difficulty in measuring the tire-road friction factor directly, meanwhile, the traditional vehicle sensors cannot provide required data at the desired accuracy. By utilizing the advanced vehicle sensors on AVs, such as video cameras, lidar sensors, GPS sensors, an Inertia Measurement Unit (IMU), we can get the vehicle and tire dynamic in real-time, such as tire normal load, tire slip ratio, and slip angle, thus the performance of the active/ passive vehicle safety system can be significantly improved.

Existing studies can be divided into two categories, such as experiment-based study, and model-based study[7]. The experiment-based study seeks to build a correlation between the sensor data and the tire-road friction[8], [9], [10]. The model-based method estimates the friction by mathematical models [11], [12], [13]. However, these methods cannot provide satisfying results. The experiment-based method is not repeatable when the experiment condition changes dramatically, and the model-based method will draw different slip-slop curves when tire condition (e.g., tire pressure, and tire wear) changes. Thus, we bring up a state-of-the-art physical informed neural network-based method to estimate the tire-road friction. Our method

incorporates the accuracy of the physically informed neural network and the simplicity of the slip-based tire model to perform a quick and accurate tire-road friction estimation.

The rest of the report is organized as follows. Section 2 explains the formation of the physical informed neural network models. Section 3 describes the hardware implementation details. Section 4 presents the experiment settings and data collections. Section 5 analysis the results.

Methodology

Section 6 concludes this report.

To give the reader an overview of the process of the Tire-road friction estimation, Figure 1 shows the structure of the estimation model. Then each part will be described in detail in the following materials.

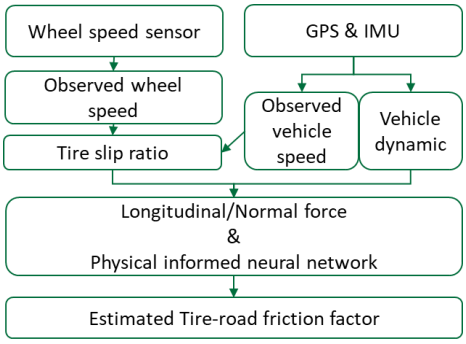

Figure 1 Model structure

Physical informed neural network

The idea of the physical informed neural network is to introduce the known differential equations into the loss function when training the neural network. This is done by sampling a set of input training data ($\{x_j\}$) and passing them through the network. Next gradients of the network's output with respect to its input are computed at these data points (which are typically analytically available for most neural networks and can be easily computed using auto-differentiation). Finally, the residual of the underlying differential equation is computed using these gradients and added as an extra term in the loss function. As shown in Figure 2.

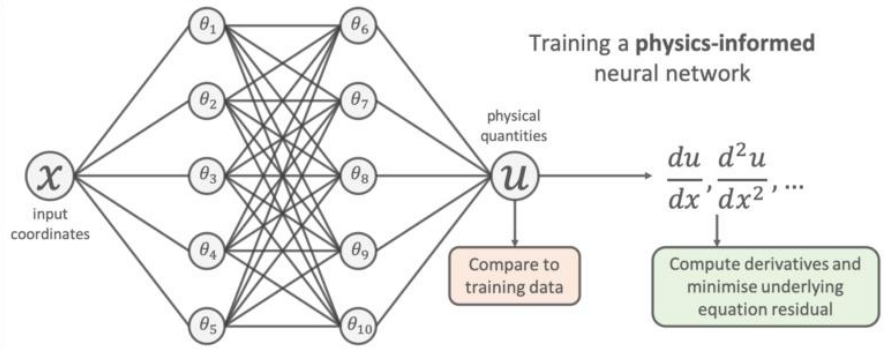

Figure 2 Scheme of physical informed neural network

The loss function of the physical informed neural network can be represented as the following equation:

$$\min \frac{1}{N}\sum_{i}^{N}\left(u_{NN}(x_i;\theta)-u_{true}(x_i)\right)^2+\frac{1}{M}\sum_{j}^{M}(\left[m\frac{d^2}{dx^2}+\mu\frac{d}{dx}+k\right]u_{NN}(x_j;\theta))$$

As you can see in the equation, the physical loss term will try to ensure that the solution learned by the network is consistent with the know physics. The physical informed neural network can predict the solution far away from the experimental data point, and thus performs better than the naïve network. On the other hand, the naive network is performing poorly because it omits some knowing scientific facts and only refers to the data at hand.

Motivated by this idea we developed a physical informed neural network model to perform fast and accurate tire-road friction factor prediction. Magic tire model and vehicle dynamics are considered in the model.

Tire model

Magical Formula (MF) is a tire formula widely used by the automotive industry which is essential to the design of the vehicle stability control system. Even the racing department will use this magic formula to design their torque control algorithm. It was named the "magic" because there is no physical basis for the formula structure, but it fits a wide variety of tire construction and operation condition. It builds a relationship between slip ratio and horizontal force. The general form of MF, given by Pacejka [14] is:

$$y = D * \sin\{C * \arctan[Bx - E * (Bx - \arctan(Bx))]\}$$

Where B, C, D, and E represent fitting constant which depends on chassis setting and tire feature. y is a force or moment resulting from a slip ratio x.

Figure 3 gives an example of a magic formula curve. Slip angle is the angle between a rolling wheel's actual direction of travel and the direction towards which it is pointing. When a vehicle runs in a straight lane, the slip angle can be assumed zero.

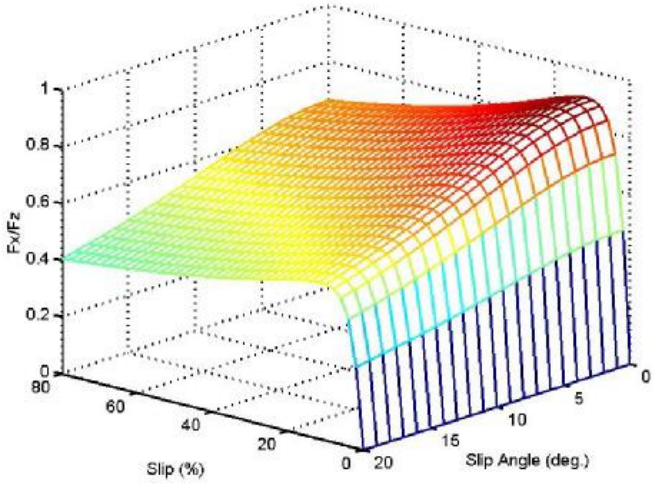

Figure 3 Example magic formula curve

Slip-ration based model

As Figure 4 shows, the $\frac{F_x}{F_z}$ is an increasing function of slip ratio until a critical value where $\frac{F_x}{F_z}$ equal to fraction factor μ, and then starts decreasing slowly. In most of our daily driving activities, particularly, for our purpose, the slip ratio is always in the increasing area. In this region, the relationship between slip and $\frac{F_x}{F_z}$ can be seen as linear. Thus, we have

$$\frac{F_x}{F_z} = K\sigma_x$$

Where σ_x is slip ratio, K is called slip-slope. According to Rajamani's [11] research, K varies as road friction coefficient changes. A linear relationship was built and calibrated with experimental data.

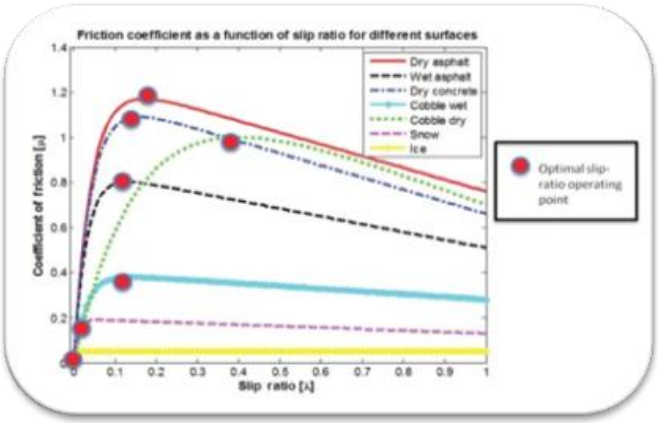

Figure 4 The Slip and Normalized longitudinal force

Vehicle dynamics

1. The definition of slip ratio:

$$\sigma_x = \frac{r_{eff}w_w - V_x}{V_x}, \quad a < 0$$

$$\sigma_x = \frac{V_x - r_{eff}w_w}{V_x}, \quad a \geq 0$$

Where,

r_{eff} is the effective radius of the tire

w_w is wheel speed

V_x is vehicle speed

The technical difficulty in this part is how to get the real vehicle speed. The most used method for not full-wheel drive vehicles is using the driven wheel to get the real vehicle speed, e.g., for a front-wheel-drive vehicle, the average wheel speed between two rear tires can be used as the real vehicle speed. Another available option is using Gyro and high-definition GPS to obtain the real vehicle speed. Based on our observation, at low speed, the GPS data is more accurate than the driven wheel data, and at high speed, the driven wheel data is more accurate. One possible reason is that most auto manufacturers use Hall sensors to get the wheel speed data which is not accurate when the speed is low. On the other hand, it is the natural characteristic for GPS data

that the accuracy will decrease with vehicle speed increases, because for a determined GPS sample rate, when the vehicle speed increases, the GPS data point is getting sparse, and thus have worse accuracy. In our experiment, both methods are employed. Determined by the driven wheel speed, when it is less than or equal to 25 mph, we will use GPS data to calculate the real vehicle speed, when it is greater than 25 mph, we will use driven wheel speed as the real vehicle speed.

2. Normal force calculation

During operation, since the vehicle will have acceleration and deceleration, the normal force of each tire usually is not a constant. Figure 5 shows the vehicle longitudinal dynamic.

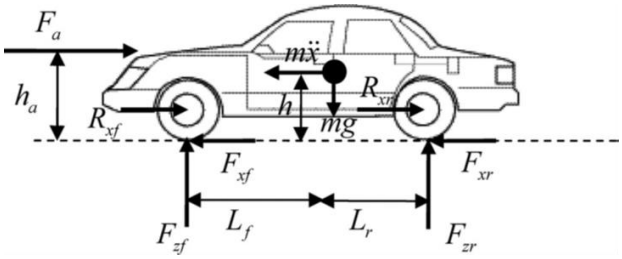

Figure 5 Longitudinal vehicle dynamic

If the vehicle is traveling in a straight line without gradient, the normal force of each tire can be calculated using the following equations:

$$F_{zf} = \frac{mgL_r - m\ddot{x}h - C_a\dot{x}^2h_a}{L}$$

$$F_{zr} = \frac{mgL_f + m\ddot{x}h + C_a\dot{x}^2h_a}{L}$$

Where,

F_{zr} and F_{zf} is the normal force of the rear axle and front axle

m is vehicle mass

L is wheelbase

L_r and L_f are rear wheel and front wheel's distance to the center of mass

C_a is aerodynamic drag parameter

h_a is the height of equivalence point of aerodynamic drag

h is the height of the center of mass

Assume the weight of the left and right sides are evenly distributed, then the normal load for each tire can be obtained.

3. Longitudinal force calculation

For each wheel, the rotation dynamic is given by

$$I_w\dot{w_w} = T_d - T_b - r_{eff}(F_x - R_x)$$

Where,

I_w is the moment of inertia of each tire

T_d and T_b is drive and brake torque for each tire. Usually, T_d can be obtained from ECU. T_b will need to be calibrated for each vehicle.

R_x is rolling resistance

Hardware Implementation

This section introduces the implementation details of the data collection AV and

This section introduces the implementation details of the AV testbed and advanced vehicle sensors.

The USF L3 automated and connected vehicle is the major equipment we have in this project. It is equipped with advanced vehicle sensors; Figure 7 shows the list of those sensors. Note that the OBD II scanner is used to read and storage the wheel speed data and engine torque, the PCan system is used to send the corresponding data inquisition to the ECU. Real-time GPS positions and speeds of the experiment vehicles were collected at a sampling rate of up to 10Hz by a high-accuracy NovAtel navigation unit with antennas affixed to the rear bumpers of the vehicles. Preliminary tests indicated that the GPS receivers had a position accuracy of 0.26 m and a speed-accuracy of 0.089 m/s. The NovAtel navigation unit also integrates an Inertia Measurement Unit (IMU) which can provide the angular velocity and angular acceleration (yaw, pitch, and roll rate) of the vehicle.

Figure 6 USF L3 AV testbed

Figure 7 Advanced vehicle sensors

To validate our algorithm, we need equipment that can provide the ground truth of road friction value, and thus we configured the USF runway Friction tester, as shown in Figure 8.

Figure 8 USF runway friction tester

Field experiment settings

As shown in Figure 9, the experiments were conducted at the segment of Florida State Rd 56 between Bruce B Downs Blvd and Gall Blvd. The length of the experiment site is around 10 miles. The building density around the road is relatively low and thus the GPS receivers have good communication with satellites. The road pavement of the road is cement concrete pavement, and the weather is sunny when we collect the data.

Figure 9 Experiment site illustration

During the experiment, both the USF runway friction tester and USF L3 AV testbed will drive through the test site. To prevent any influence from whether, e.g., rain, wind, these two cars will operate simultaneously, i.e., one car follows another one. When the USF runway friction tester work, it will spray water to the pavement to prevent the rubber tire from getting burned, which is used to collect the road friction factor. Considering this fact, this friction tester needs to follow the USF L3 AV testbed to collect data.

To study the influence of vehicle speed as well as the vehicle dynamic on the accuracy of prediction, we collected data on different speed ranges with speed changes during the experiment. For illustration purposes, the five-speed profiles are shown in Table 1. It is observed that each speed profile is composed of three periods. In the first period (0s-30s), the lead vehicle cruised with an initial speed (varying from 15 mph to 35 mph, which is the speed limit of the Road friction tester during data collection). In the second period (30s-60s), the lead vehicle decreased its speed to a target speed (vary from 10 mph to 30 mph) and remained the target speed till the end of this period. In the third period (60s-90s), the lead vehicle increased its speed to the initial speed and maintained the initial speed till the end of the third period, which indicates the accomplishment of one test. In each profile, the leading vehicle speed will decrease

by 5 mph. The following vehicle, i.e., the road friction tester, will be driven by an experienced driver and always maintain a safe distance from the proceeding vehicle.

Table 1 Speed profile of the experiment vehicles

Speed Profile	0s-30s	30s-60s	60s-90s
1	35 mph	30 mph	35 mph
2	30 mph	25 mph	30 mph
3	25 mph	20 mph	25 mph
4	20 mph	15 mph	20 mph
5	15 mph	10 mph	15 mph

Result Analysis

More than 15,000 data points are collected for different speed ranges during the experiment. Figure 10 gives an example of the prediction result on one of the driving wheels for speed profile 1. As described in the figure, a lot of outliers are observed in the data. There are two possible reasons. One possible reason could be the accumulated spin error of IMU, which will lead to an abnormal normal force for individual tires, and thus lead to a higher slip-slop K, then higher road friction factor. Another possibility is the sampling error of the Hall wheel speed sensor, to address this issue and get a more accurate prediction, a grating displacement sensor or ultrasonic position sensor is needed to be integrated. Let alone those outliers, most of the maximum friction factor along the time axes is located between 0.1 and 0.6 with a mean at 0.38. Referring to [15], this range is reasonable for a cement concrete pavement road on sunny days.

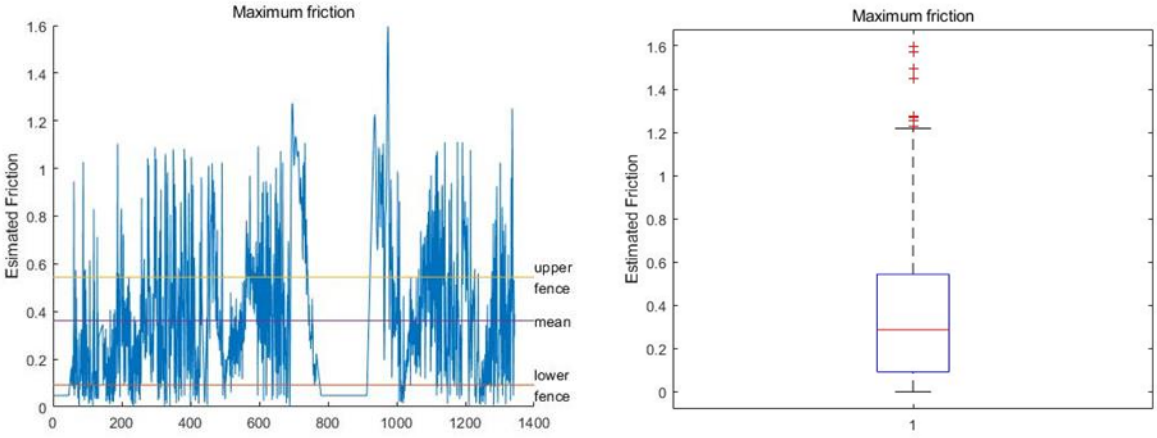

Figure 10 Example prediction result of speed profile 1

One may notice the maximum friction factor remains constant between 800 and 900 data points. The reason for this phenomenon is that the data collection is performed on the public road, and there are few signalized intersections in the test site. During this specific period, the road friction tester and the USF L3 AV testbed are stopped, and thus the output of slip ratio, as well as the vehicle speed, is zero, then the model will output a constant 0.05, which is served as a correction term in the model.

Conclusion

This project investigated the possibility of using a vehicular sensor to detect the tire-road friction factor which is critical to the design and tunning of the active and passive vehicle stability controls. During this project, we have reviewed the previous work in tire-road friction factor detections and categorized them into model-based method and experiment-based method. Both methods have it pros and cons, and most of them cannot provide an accurate prediction when the environmental conditions change dramatically. To address this gap, a physical informed neural network based model was developed to predict the tire-road friction factor. This model absorber both advantage of the experiment-based method and model-based method, it is aware of the characteristics of tires and meanwhile can take advantage of massive experiment data. This model was applied to the USF L3 AV testbed equipped with advanced vehicle sensors to collect and validate our algorithms. The USF runway friction tester was employed as ground truth to provide 'real' road friction factors. During the experiment, we found that the physical informed neural network model can be applied to various speed ranges and can get desirable prediction results, which show its reliability in different speed conditions. However, due to the limitation of the test site and the uncertainty of the weather condition during the environment, we didn't collect data in wet pavement conditions. So, it is unknown to us whether the performance of the model will stay consistent in rainy conditions. Additionally, with physical facts involved in the loss function of network training, the convergence can be reached at a short time compared to a naive network. Meanwhile, outliers are observed in the output. Two possible reasons are identified. One possible reason could be the accumulated spin error of IMU, which will lead to an abnormal normal force for individual tires, and thus lead to a higher slip-slop K, then higher road friction factor. Another possibility is the sampling error of the Hall wheel speed sensor. Thus, we can further expand the work of this project by adding more accurate sensors and performing the experiment in different pavement conditions, e.g., wet pavement, and different pavement types, e.g., hot mix asphalt, stone mastic asphalt, composite.

References

[1] X. Li, J. Cui, S. An, and M. Parsafard, "Stop-and-go traffic analysis: Theoretical properties, environmental impacts and oscillation mitigation," *Transp. Res. Part B Methodol.*, vol. 70, no. C, pp. 319–339, 2014, doi: 10.1016/J.TRB.2014.09.014.

[2] F. Zhou, X. Li, and J. Ma, "Parsimonious shooting heuristic for trajectory design of connected automated traffic part I: Theoretical analysis with generalized time geography," *Transp. Res. Part B Methodol.*, vol. 95, pp. 394–420, Jan. 2017, doi: 10.1016/J.TRB.2016.05.007.

[3] X. Qu, Y. Yu, M. Zhou, C. T. Lin, and X. Wang, "Jointly dampening traffic oscillations and improving energy consumption with electric, connected and automated vehicles: A reinforcement learning based approach," *Appl. Energy*, vol. 257, p. 114030, Jan. 2020, doi: 10.1016/J.APENERGY.2019.114030.

[4] H. Yao, J. Cui, X. Li, Y. Wang, and S. An, "A trajectory smoothing method at signalized intersection based on individualized variable speed limits with location optimization," *Transp. Res. Part D Transp. Environ.*, vol. 62, pp. 456–473, Jul. 2018, doi: 10.1016/J.TRD.2018.03.010.

[5] S. E. Li, R. Li, J. Wang, X. Hu, B. Cheng, and K. Li, "Stabilizing Periodic Control of Automated Vehicle Platoon with Minimized Fuel Consumption," *IEEE Trans. Transp. Electrif.*, vol. 3, no. 1, pp. 259–271, Mar. 2017, doi: 10.1109/TTE.2016.2628823.

[6] Z. Wadud, D. MacKenzie, and P. Leiby, "Help or hindrance? The travel, energy and carbon impacts of highly automated vehicles," *Transp. Res. Part A Policy Pract.*, vol. 86, pp. 1–18, Apr. 2016, doi: 10.1016/J.TRA.2015.12.001.

[7] S. Khaleghian, A. Emami, and S. Taheri, "A technical survey on tire-road friction estimation," *Friction*, vol. 5, no. 2, pp. 123–146, 2017, doi: 10.1007/s40544-017-0151-0.

[8] F. Gustafsson, "Slip-based tire-road friction estimation," *Automatica*, vol. 33, no. 6, pp. 1087–1099, 1997, doi: 10.1016/s0005-1098(97)00003-4.

[9] J. Matuško, I. Petrović, and N. Perić, "Neural network based tire/road friction force estimation," *Eng. Appl. Artif. Intell.*, vol. 21, no. 3, pp. 442–456, 2008, doi: 10.1016/j.engappai.2007.05.001.

[10] Y. H. Liu, T. Li, Y. Y. Yang, X. W. Ji, and J. Wu, "Estimation of tire-road friction coefficient based on combined APF-IEKF and iteration algorithm," *Mech. Syst. Signal Process.*, vol. 88, no. July 2016, pp. 25–35, 2017, doi: 10.1016/j.ymssp.2016.07.024.

[11] R. Rajamani, G. Phanomchoeng, D. Piyabongkarn, and J. Y. Lew, "Algorithms for real-time estimation of individual wheel tire-road friction coefficients," *IEEE/ASME Trans. Mechatronics*, vol. 17, no. 6, pp. 1183–1195, 2012, doi: 10.1109/TMECH.2011.2159240.

[12] T. Y. K. and S. H. LEE, "ESTIMATION OF MAXIMUM ROAD FRICTION COEFFICIENT BASED ON LYAPUNOV METHOD," *Int. J. …*, vol. 13, no. 2, pp. 293–300, 2012, doi: 10.1007/s12239.

[13] S. Müller, M. Uchanski, and K. Hedrick, "Estimation of the Maximum Tire-Road Friction Coefficient," *J. Dyn. Syst. Meas. Control. Trans. ASME*, vol. 125, no. 4, pp. 607–617,

2003, doi: 10.1115/1.1636773.

[14] H. B. Pacejka and E. Bakker, “THE MAGIC FORMULA TYRE MODEL,” *http://dx.doi.org/10.1080/00423119208969994*, vol. 21, no. sup1, pp. 1–18, Jan. 2007, doi: 10.1080/00423119208969994.

[15] G. Flintsch, E. Izeppi, K. McGhee, and S. Najafi, “The little book of tire pavement friction. Surface Properties Consortium,” no. September, pp. 0–22, 2012.